Journal of Particle Science and Technology 5 (2019) 47-60

J | P | S | T

http://jpst.irost.ir

Journal of Particle Science and Technology

IROST

Surface decorated magnetite nanoparticles with birhodanine and $MoO_2Cl_2(dmf)_2$ as a new magnetic catalyst for epoxidation of olefins

Arman Rahmaninia, Yagoub Mansoori*, Farough Nasiri*, Abolfazl Bezaatpour, Behnam Babaei

Department of Applied Chemistry, Faculty of Science, University of Mohaghegh Ardabili, Ardabil, Iran

HIGHLIGHTS

- Synthesis and characterization of a new magnetically supported Mo^{6+} complex nanoparticles have been reported and used as catalyst.
- The catalyst was used for the epoxidation of olefins, using cyclooctene as a model substrate to optimize the reaction conditions.
- The catalyst showed excellent conversions, good turn over frequencies, and short reaction times for the epoxidation of olefins.

GRAPHICAL ABSTRACT

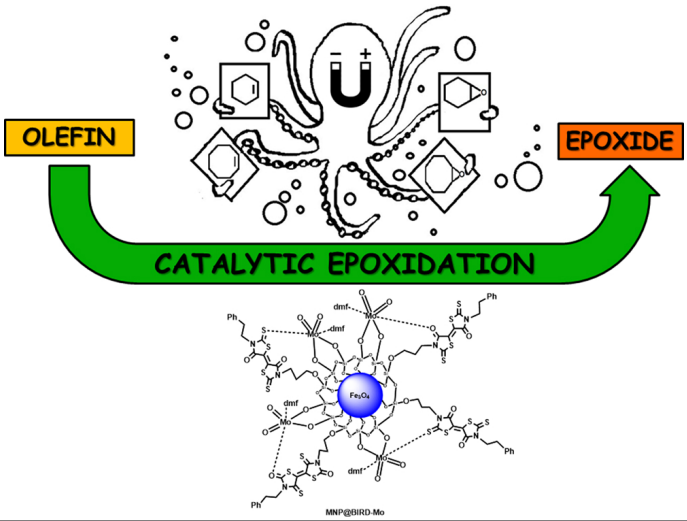

ARTICLE INFO

Article history:

Received 29 November 2018
Revised 23 January 2019
Accepted 9 February 2019

Keywords:

Magnetic Nanoparticles
Birhodanine
$MoO_2Cl_2(dmf)_2$
Silylation

ABSTRACT

In this work, the synthesis and characterization of a new magnetically supported Mo^{6+} complex have been reported as a catalyst for epoxidation of olefins. For this purpose, a new silylating compound containing a birhodanine moiety, i.e. [(E)-5-(3-(3-(trimethoxysilyl)propyl)-4-oxo-2-thioxothiazolidin-5-ylidene)-3-phenethyl-2-thioxothiazolidin-4-one] (TMOS-BIRD) has been synthesized and used for silylation of magnetite nanoparticles (MNPs). The magnetically supported catalyst was then prepared by deposition of dioxomolybdenum(VI) adduct, dichlorobis(dimethylformamide) dioxomolybdenum ($MoO_2Cl_2(dmf)_2$), on MNP@BIRD. The prepared supported magnetic catalyst was characterized in detail by FT-IR, transmission electron microscopy (TEM), thermogravimetric analysis (TGA), X-ray diffraction (XRD), vibrating sample magnetometry (VSM) and energy-dispersive X-ray (EDX) analyses. Cyclooctene was used as a model substrate to optimize the epoxidation reaction conditions, and the prepared magnetically retrievable catalyst was then used for epoxidation of cyclohexene, cyclooctene, styrene, indene, *trans-trans-cis*-1,5,9-cyclododecatrien, 1-octene, 1-heptene, α-pinene, 1-dodecene and *trans*-stilbene using *tert*-butyl hydroperoxide (TBHP) as oxidant under solvent-free conditions. The catalyst showed excellent conversion, good turn over frequency, and a short reaction time at 95 °C for epoxidation of cyclooctene.

* Corresponding author: Tel.: +9845-31505205 ; Fax: +9845-33514701 ; E-mail address: ya_mansoori@uma.ac.ir

DOI: 10.22104/JPST.2019.3321.1141

1. Introduction

As a very important class of organic chemicals, epoxides have attracted a great deal of attention from an industrial point of view. They are significant starting materials for industrially valuable products such as drugs, epoxy resins, intermediates and surfactants [1,2]. In recent decades, epoxidation of olefins by transition metal complexes has been regarded as the conventional route [3]. Dileep and Rudresha reported the synthesis of an immobilized copper complex onto 1-ethyl-3-methylimidazolium hexafluorophosphate, as an ionic liquid support, for epoxidation of olefins [4]. The solubility of hydrogen peroxide (oxidant) and catalyst in the ionic liquid and easy separation of the products by extraction are the main advantages of their oxidation system. Shi et al. reported two new inorganic–organic hybrids, based on Co(II) and Ni(II) for oxidation of styrene [5]. Recently, Uozumi and Osako reported the epoxidation of olefins by ruthenium-exchanged hydroxyapatite in the presence of O_2 [6]. Among the various catalysts reported for epoxidation of olefins, Mo6+ complexes have distinct advantages such as stability, commercial availability and environment-friendliness in catalysis of epoxidation reactions [7-9].

Despite high reactivity, insufficient chemical and thermal stability of catalysts and catalysts recycling are two main difficulties of homogeneous catalysts. These problems may be solved by supporting homogeneous catalysts on polymers [10], metal oxides, and in particular different nanomaterials [4,11,12] which have attracted increasing attention in recent years. Among the inorganic materials used for this purpose, functionalized MNPs exhibit the advantages of biocompatibility, easy recovery by magnetic separation, thermal stability, large surface area and high capacity of active sites for loading [13].

Birhodanines, as an interesting group of rhodanine-based derivatives, can be synthesized through various routes [14]. Applications of these organic heterocycles have been extended across numerous fields such as dyes [15], transistors [16], catalysts [17,18], polymers and nanocomposites [19]. The coordinating ability of birhodanines with different metallic ions has also been noted, since they have several potentially coordinating sites in their structure [20-25].

Following our reported approach to simple, solvent-free and one-pot synthesis of birhodanine compounds [26,27] and considering the coordination ability of rhodanine ring toward metal ions, in this study a birhodanine containing silane compound, TMOS-BIRD, is synthesized and used for silylation of a MNPs surface. Complex $MoO_2Cl_2(dmf)_2$ is one of the solvent adducts with the general formula $MoO_2X_2(S)_2$ (X = F, Cl, Br; S = thf, dmf, dmso, CH_3CN, H_2O). It has been used in several organic transformations such as epoxidation of olefins, oxidation of alcohols, and reductive cyclization of nitrobiphenyls and nitrostyrenes to carbazoles and indoles [28]. In this regard, Monteiro et al. investigated the use of $MoO_2Cl_2(dmf)_2$-supported on MCM-41 for epoxidation of olefins [28]. Our prepared catalyst showed a similar conversion for epoxidation of cyclooctene (~97%), but within a shorter reaction time with respect to the $MoO_2Cl_2(dmf)_2$-supported on MCM-41. The influence of reaction conditions such as amount of catalyst, reaction time, substrate:oxidant molar ratio temperature, type of oxidant, temperature, and solvent was investigated for epoxidation of cyclooctene as the model reaction. The catalyst performance for epoxidation of various olefins in the presence of *t*-BuOOH under optimal conditions is shown, and the catalyst was recovered by simple magnetic decantation upon completion of the reaction. To the best of our knowledge, the present work is the first report on rhodanine derivatives as a magnetically supported ligand for catalytic application.

2. Experimental

2.1. Instruments

The FT-IR (KBr) spectra were recorded on a PerkinElmer RXI spectrophotometer. NMR spectra were obtained on a Bruker Avance 250 MHz spectrometer using tetramethylsilane (TMS). TGA curves were obtained on a Linseis STA PT 1000 instrument with the scanning rate of 10°C/min. Atomic absorption spectroscopy was performed on a Analytik Jena NovaAA 400. A Philips (X-Pro) X-ray diffractometer equipped with Ni-filtered Cu-K_α radiation source was used for XRD measurements at room temperature with the scanning rate of 1°/min over a 2θ range of 10–80°. The TEM image of the silylated nanoparticles was obtained on a Philips EM208. Dispersing of the nanoparticles was done in an ultrasonic bath (Parsonic 7500S). A vibrating sample magnetometer (VSM,

Maghnatis Danesh-pajooh Kashan Co., Iran) with a maximum magnetic field of 10 kOe was used for magnetization measurements at room temperature. The multi point N_2 adsorption/desorption analysis according to the BET (Brunauer-Emmett-Teller) method was performed at -197.018 °C using a TriStar II plus Micromeritics automated gas adsorption analyzer. Gas chromatography (GC) was used for the oxidation analysis using Agilent 7890 A. The instrument was equipped with a flame ionization detector and a capillary column. The temperature of the column was programmed between 180 and 200 °C with 2 °C/min rate.

2.2. Materials

Magnetite nanoparticles, $MoO_2Cl_2(dmf)_2$ and methyl 2- (4-oxo -3-phenethyl -2-thioxothiazolidin -5-ylidene) acetate (IV) were prepared according to the methods described in the literature [28-30]. The other chemicals and solvents were of laboratory grade, obtained from Merck Co. and used without further purification.

2.3. Synthesis of the silylating birhodanine compound (TMOS-BIRD)

A mixture of APTMS (0.358 g, 1 mmol), carbon disulfide (0.304 g, 4 mmol), compound IV (0.616 g, 2 mmol), and a catalytic amount of tetrabutylammonium bromide (TBAB) (0.128 g, 0.4 mmol) was stirred for 1 h at room temperature under solvent-free condition. Then, water (8 ml) and dichloromethane (32 ml) were added, and the organic layer was separated and dried over anhydrous calcium chloride. Finally, EtOH was used to recrystallize the crude product in order to afford 0.316 g golden crystals (Yield: 30%). M.p. 205-207°C. FT-IR (KBr, cm^{-1}): 2927 (m), 1695 (s), 1428 (m), 1349 (s), 1176 (s), 1086 (s), 870 (m), 743 (m), 699 (m). ^{1}H-NMR (250 MHz, $CDCl_3$) δ (ppm): 7.26-7.31 (m, J = 5 Hz, 5H), 4.33 (t, J = 7.5 Hz, 2H), 4.11 (t, J = 7.5 Hz, 2H), 3.56 (s, 9H), 2.99 (t, J = 7.8 Hz, 2H), 1.70-2.00 (m, 2H), 0.67 (t, J = 7.5 Hz, 2H). ^{13}C-NMR (62.5 MHz, $CDCl_3$) δ (ppm): 194.2, 166.6, 136.8, 128.7, 127.0, 124.9, 124.3, 50.6, 46.7, 45.6, 33.0, 20.5, 13.7, 6.5.

2.4. Silylation of magnetite and synthesis of MNP@BIRD

To immobilize BIRD on the MNPs, TMOS-BIRD (0.700 g, 1.3 mmol) was added to the MNPs (0.600 g in 30 ml) dispersed in a toluene solution of triethylamine (6.0 ml, 2M) and stirred for 24 h under argon atmosphere at room temperature. The silylated MNPs were decanted magnetically, washed with 20 ml of MeOH, re-dispersed in toluene and washed with MeOH. Removal of any un-reacted TMOS-BIRD was ensured by repeating the washing procedure three times, and finally, the silylated nanoparticles were dried in vacuum [31].

2.5. Epoxidation of alkenes by MNP@BIRD-Mo

Epoxidation of various alkenes was conducted using MNP@BIRD-Mo as a magnetic heterogeneous catalyst. Typically, in a round-bottom flask, 9.5 mg of MNP@BIRD-Mo (1.5 mol%) were dispersed in freshly distilled cyclooctene (0.5 mmol, 58 µl) in an ultrasonic bath. TBHP (80% solution in *tert*-butylhyroperoxide–water, 1.0 mmol, 143.1 µl) and internal standard (1,2-dichlorobenzene, 0.5 mmol) were added, and the mixture was stirred for 10 minutes at 95 °C under solvent-free conditions. The catalyst was separated magnetically, washed with n-hexane dried in a vacuum oven at 40 °C, and the residue was analyzed by GC to determine its final oxidation products.

3. Results and discussion

3.1. Synthesis and characterization of MNP@BIRD-Mo nanoparticles

The silylating birhodanine compound TMOS-BIRD (VI) was prepared according to Scheme 1. Methyl 2-(4- oxo-3- phenethyl-2- thioxothiazolidin-5- ylidene) acetate (IV) was simply obtained (58% yield) through a one pot three component reaction of 4-phenetylamine (II), carbon disulfide (I), and DMAD (III) in water at room temperature. It was then further reacted with carbon disulfide (I) and (3-aminopropyl)trimethoxysilane (V) in the presence of tetrabutylammonium bromide (TBAB) under solvent-free conditions at room temperature to give TMOS-BIRD (VI) [30]. Common spectroscopy methods were applied to confirm the structure of TMOS-BIRD. Figs. 1(a) and 1(b) present the ^{1}H-NMR and ^{13}C-NMR spectra of TMOS-BIRD, respectively. As Fig. 1(a) shows, the aromatic ring protons of TMOS-BIRD appear at 7.20 to 7.40 ppm, while the protons related to the methylene groups are distinguished with the expected multiplicities. In Fig. 1(b), the observed

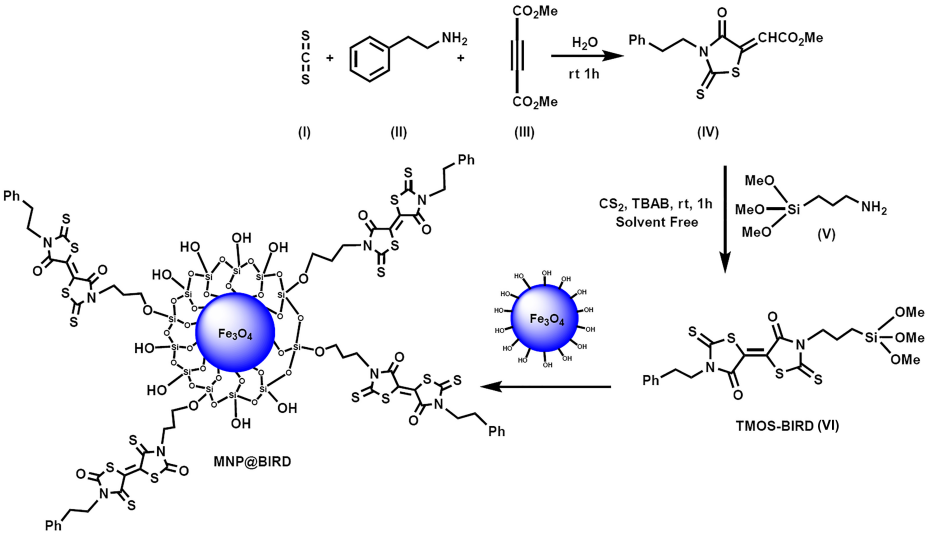

Scheme 1. Synthesis of MNP@BIRD nanoparticles.

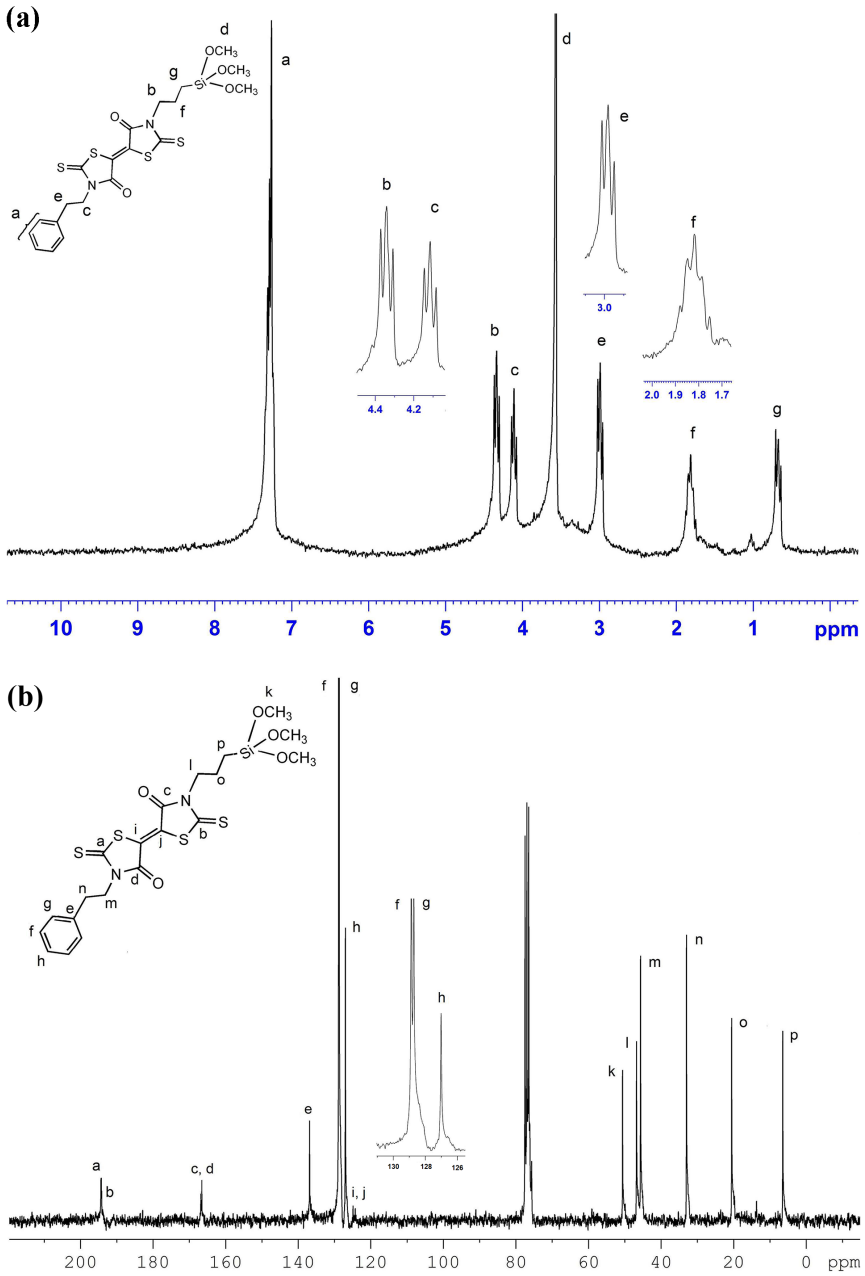

Fig. 1. (a) ^{1}H-NMR (250 MHz, $CDCl_3$), and (b) ^{13}C-NMR (62.5 MHz, $CDCl_3$) of TMOS-BIRD (VI).

16 signals are compatible with the structure of TMOS-BIRD. In the mass spectrum (Fig. 2), a molecular ion peak appears at m/e = 528.2 (16%).

As Scheme 1 shows, the nanoparticles of MNP@BIRD were obtained through silylation of MNPs by TMOS-BIRD. Figs. 3(a) to 3(c) show the FT-IR spectra of the MNPs, the MNP@BIRD, and TMOS-BIRD, respectively. In the FT-IR spectrum of the MNP@BIRD (Fig. 3(b)), appearance of 3030 cm^{-1} (νs arom. C-H), 2928 cm^{-1} (νs CH_2), 1696 cm^{-1} (C=O stretching) and 1428 cm^{-1} (CH_2 bending) transmittance bands, along with the rhodanine ring related vibrations at 1350, 1262, and 1176 cm^{-1}, clearly confirms silylation of the MNPs by TMOS-BIRD. The presence of the νas Si-O-Si vibrational mode at 1112 cm^{-1} in addition to the characteristic peak of magnetite at 588 cm^{-1} [32] confirms success of the silylation reaction.

Exposure of magnetic nanoparticles of MNP@BIRD to a dichloromethane solution of $MoO_2Cl_2(dmf)_2$ gave supported Mo^{6+}, Scheme 2. The amount of loaded Mo^{6+} (0.80 $mmol.g^{-1}$; 7.65 wt%) was measured by atomic absorption spectroscopy. Therefore, the average surface coverage of the supported catalyst is 2.6 atom Mo/nm^2 based on the metal loading of 0.80 $mmol.g^{-1}$ and a surface area of 188 $m^2.g^{-1}$ (obtained from the BET measurement).

Figs. 4(a) and 4(b) show the FT-IR spectra of the MNP@BIRD and the supported Mo^{6+} complex, respectively. As it can be seen, the C=O stretching band

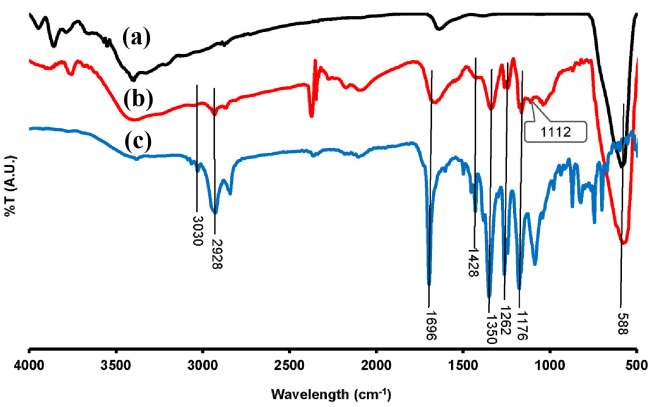

Fig. 3. The comparative FT-IR spectra of (a) MNPs, (b) MNP@BIRD, and (c) TMOS-BIRD (VI).

shifted to lower frequencies by 34 cm^{-1} and appeared at 1652 cm^{-1} along with the C=O frequency of dmf [28]. This can be attributed to weakening of C=O bonds upon coordination to Mo^{6+}. The adsorption bands observed at 910 and 950 cm^{-1} can be assigned to asymmetric and symmetric Mo=O stretching vibrations with a distorted octahedral geometry and a *cis*-dioxo unit [33].

The TEM image of MNP@BIRD supported Mo^{6+} complex reveals spherical nanoparticles of uniform size distribution (20-30 nm) as seen in Fig. 5.

Figs. 6(a) and 6(b) present the XRD patterns of the bare MNPs, MNP@BIRD, and MNP@BIRD-Mo, respectively. These figures outline the characteristic peaks of magnetite. Therefore, Fig. 6(a) confirms the formation of cubic magnetite nanoparticles (JCPDS-ICDD Copyright 1938, file No. 01-1111) with the

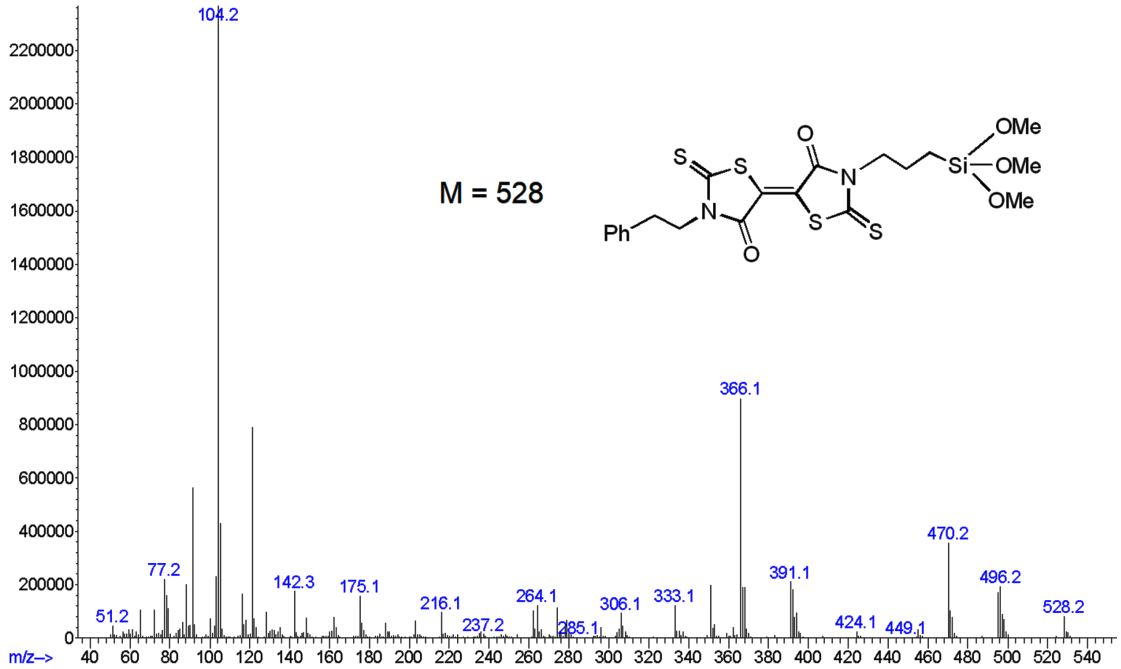

Fig. 2. Mass spectrum of TMOS-BIRD (VI).

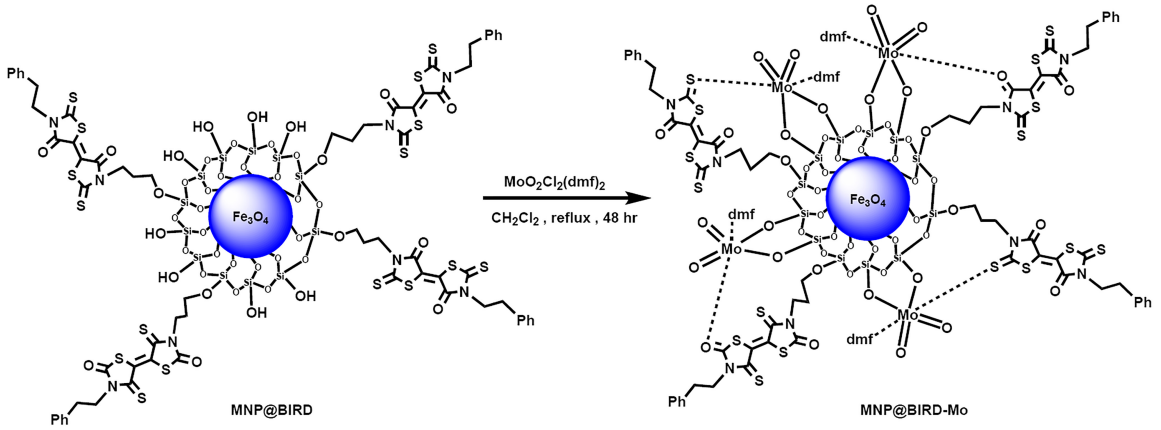

Scheme 2. Supporting of Mo^{6+} complex on MNP@BIRD nanoparticles.

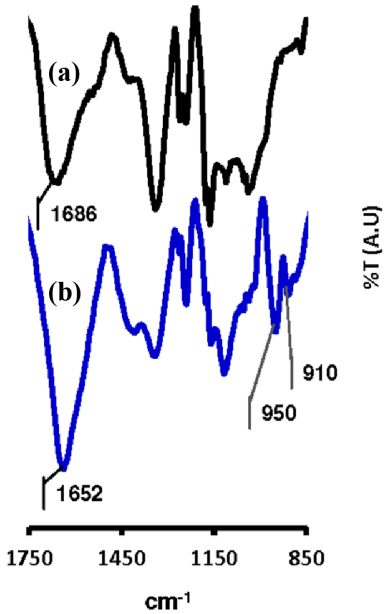

Fig. 4. Portion FT-IR spectra of (a) MNP@BIRD and (b) MNP@BIRD-Mo.

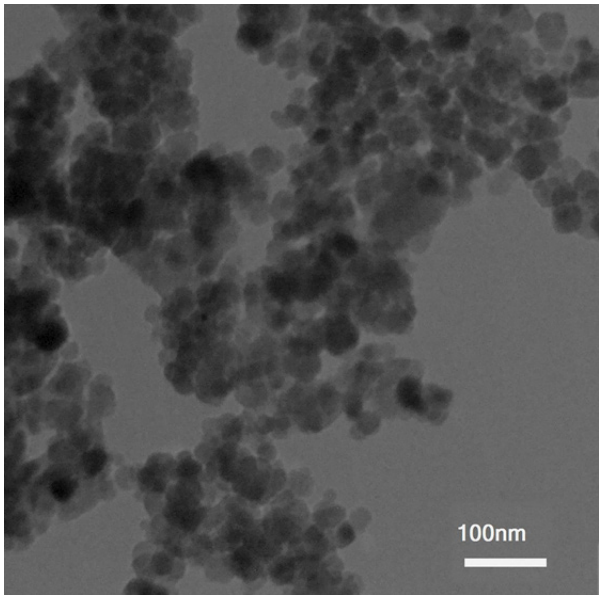

Fig. 5. TEM image of MNP@BIRD-Mo catalyst.

Fd-3m space group [34]. Furthermore, the crystal structure of magnetite remained unchanged in the final nanoparticles, and the diffraction peaks of the supported catalyst are relatively attenuated due to the coating of MNPs by an amorphous silica and catalyst supporting, Fig. 6(b).

Fig. 7 depicts the magnetization curves of the MNPs, MNP@BIRD, and MNP@BIRD-Mo, and Table 1 summarizes the results. As it can be seen, the saturation magnetization values (M_s) of the prepared nanoparticles are in the range of 52.0 to 78.1 emu.g^{-1}. The values are less than the values reported for bulk magnetite particles (92 to 100 emu.g^{-1}) due to the superparamagnetism behavior that can be observed for single domain magnetic nanoparticles below a critical size [35]. The formation of a non-magnetic silica layer around the MNPs and supporting of Mo^{6+} complex are responsible for decreasing the M_s values. Moreover, small field coercivity of the supported complex (H_c = 29.7 Oe, M_r = 2.4 emu.g^{-1} and M_r/M_s = 0.05) shows that the nanoparticles of the supported catalyst are superparamagnetic [36].

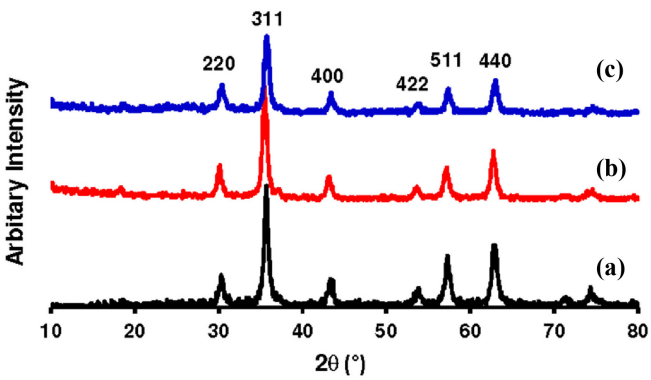

Fig. 6. XRD patterns of (a) MNPs, (b) MNP@BIRD and (c) MNP@BIRD-Mo complex.

Table 1. Magnetic properties of MNPs, MNP@BIRD and MNP supported Mo^{6+} complex.

Sample	M_s (emu.g^{-1}) [a]	M_r (emu.g^{-1}) [b]	H_c (Oe) [c]	M_r/M_s [d]
MNP	78.1	3.8	18.6	0.05
MNP@BIRD	69.5	3.8	36.5	0.05
MNP@BIRD-Mo	52.0	2.4	29.7	0.05

[a] Saturation magnetization. [b] Remanent magnetization. [c] Coercive force. [d] Remanence ratio.

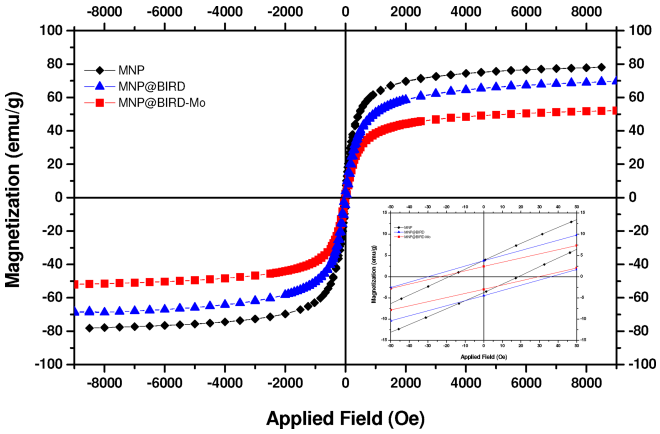

Fig.7. Magnetization curves for the MNPs, MNP@BIRD and MNP@BIRD-Mo at room temperature.

TGA was used to estimate the quantity of the loaded Mo^{6+} complex. Fig. 8(a) shows removal of physically and chemically adsorbed H_2O molecules (from ambient temperature to 200 ºC) and thermal degradation of birhodanine moiety from 200-600 ºC by a total mass loss of about 6.55% for the MNP@BIRD. Under the same condition, a very distinct mass loss of approximately 13.77% is observed for MNP@BIRD-Mo due to the thermal breakdown of the complex, Fig. 8(b). The difference between these two values (Δm = 7.22%) can be attributed to the amount of complex loaded onto the MNP@BIRD (7.73% or 77.3 mg.g^{-1} of MNP@BIRD).

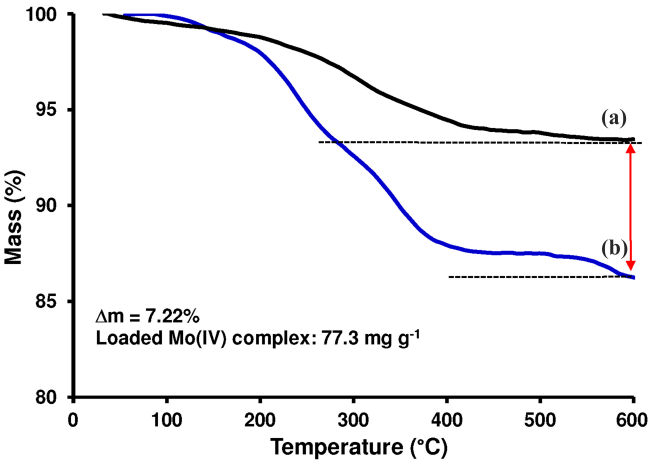

Fig. 8. TGA thermograms (N_2 atmosphere, scan rate of 10ºC/min) of (a) MNP@BIRD, and (b) MNP@BIRD-Mo complex.

Fig. 9 depicts the energy-dispersive X-ray (EDX) spectrum and EDX mappings of C K_α, Fe K_α, O K_α, N K_α, and Mo L_α of the supported Mo^{6+} complex. This experiment revealed the presence of the mentioned elements in accordance with the chemical composition of the catalyst.

3.2. Epoxidation of olefins

The reaction conditions were optimized by focusing on the epoxidation reaction of cyclooctene (0.5 mmol) by TBHP (0.5-2.5 mmol) as a model substrate, and varying the reaction parameters such as catalyst dosage (7.5-11.0 mg), reaction time (5-10 min), oxidant:substrate molar ratio (1.0-5.0), oxidant type, reaction temperature (55-95 °C) and the solvent. Table 2 summarizes the results, and Fig. 10 presents the details of finding the optimal conditions. The effect of catalyst loading, reaction time, oxidant/substrate molar ratio, and reaction temperature were optimized (Figs. 10(a) and 10(b)). The best conversion was observed by using 1.5 mol% molybdenum (9.5 mg) with the oxidant/substrate molar ratio of 2.0:1.0 over 10 min (Entry 7, 97.3% yield). TBHP showed the best reactivity among the investigated oxidants (Entries 7 to 10) at 95 °C (Entry 7, Fig. 10(c)) and the use of solvents of different polarities lowered the reaction yields (Entries 14 to 19, Fig. 10(d)). The conversion was low in the absence of catalyst (Entry 13). Therefore, 1.5 mol% molybdenum (9.5 mg), TBHP (2.0. mmol), and absence of solvent are the optimal reaction conditions for epoxidation of cyclooctene (1.0 mmol) at 95 °C during 10 min.

After optimizing the reaction conditions, the reaction scope was investigated by applying the supported Mo^{6+} nano-catalyst to the epoxidation reaction of olefins. Table 3 lists the results. As seen, the best conversion was observed for epoxidation of cyclooctene (Entry 1). Scheme 3 proposes a possible mechanism for the epoxidation reaction catalyzed by supported Mo^{6+} catalyst. As observed, reaction intermediate and electron donation from the π (C=C) of olefins into the

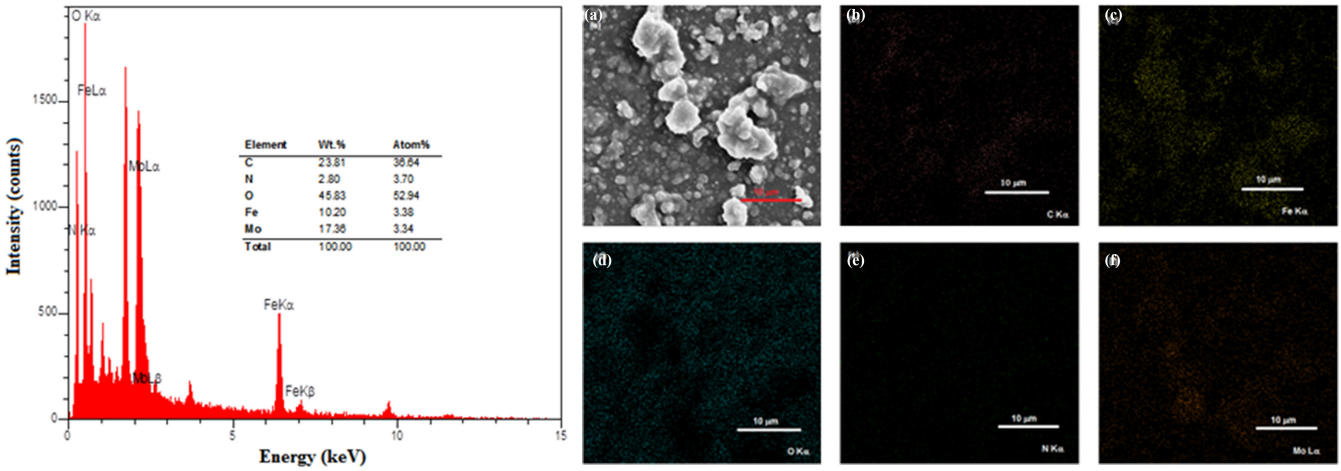

Fig. 9. EDX spectrum of MNP@BIRD-Mo complex with the quantitative data. Insets show the (a) SEM image of the catalyst, (b) The elemental maps of an aggregate using C K_a, (c) Fe K_a, (d) O K_a, (e) N K_a and (f) Mo L_a.

unoccupied σ*(O-O) orbital of peroxo group are noted in the proposed mechanism [37].

Table 4 presents a comparison of the catalytic activity of the supported Mo^{6+} complex in the epoxidation of cyclooctene to a few catalysts reported in the literature. Although, the extent of conversion in some cases are slightly higher than that of our result, with our reported nano-catalyst the conversion reaches 97% in

Table 2. Optimization of conditions for epoxidation reaction of olefins.

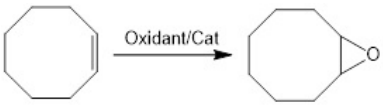

Entry	Solvent	Mo (mol%)	Oxidant	Oxidant: Substrate	Time (min)	Temperature (°C)	Conversion (%) [a]	TON [b]	TOF [c] (h^{-1})
1	-	1.2	TBHP	2.0:1.0	10	95	78	65.2	391.0
2	-	1.4	TBHP	2.0:1.0	5	95	92	67.9	815.3
3	-	1.5	TBHP	2.0:1.0	5	95	95	62.5	750.0
4	-	1.4	TBHP	2.0:1.0	10	95	96	70.7	424.0
5	-	1.5	TBHP	1.0:1.0	5	95	89	58.8	705.0
6	-	1.5	TBHP	1.5:1.0	5	95	95	62.6	751.6
7	-	1.5	TBHP	2.0:1.0	10	95	97	64.0	383.3
8	-	1.5	$NaIO_4$	2.0:1.0	10	95	0.0	0.0	0.0
9	-	1.5	H_2O_2	2.0:1.0	10	95	0.0	0.0	0.0
10	-	1.5	UHP	2.0:1.0	10	95	4.0	2.6	15.8
11	-	1.5	TBHP	2.0:1.0	10	75	50	33.0	198.2
12	-	1.5	TBHP	2.0:1.0	10	85	77	50.9	305.5
13	-	0	TBHP	2.0:1.0	10	95	40	-	-
14	Acetonitrile [d]	1.5	TBHP	2.0:1.0	10	- [e]	5	3.3	19.7
15	Chloroform [d]	1.5	TBHP	2.0:1.0	10	- [e]	13	8.6	51.3
16	Methanol [d]	1.5	TBHP	2.0:1.0	10	- [e]	25	16.4	98.7
17	Ethanol [d]	1.5	TBHP	2.0:1.0	10	- [e]	30	19.7	118.4
18	1,2-Dichloroethane [d]	1.5	TBHP	2.0:1.0	10	- [e]	40	26.3	157.9
19	Dichloromethane [d]	1.5	TBHP	2.0:1.0	10	- [e]	52	34.2	205.3

[a] Determined by GC analysis. [b] Turn over frequency: Turn over number: TON = The number of moles of desired product/The number of moles of metal active sites. [c] TOF = The number of moles of reactant converted/(The number of moles of metal active sites × Time in hours). [d] Solvent (1 mL). [e] Reflux temperature.

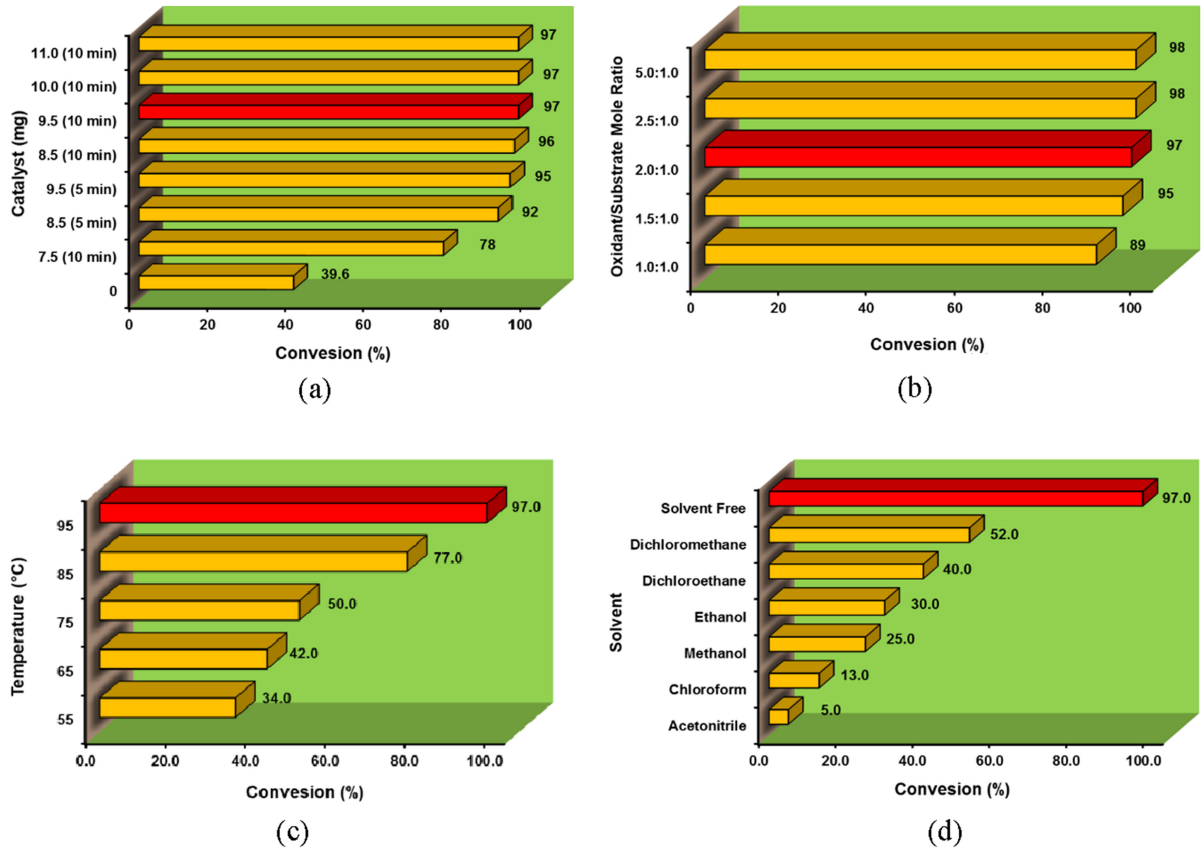

Fig. 10. Optimization of the epoxidation reaction conditions (a) Catalyst loading, (b) Oxidant/substrate molar ratio, (c) Reaction temperature and (d) Solvent. Reaction conditions: cyclooctene (1.0 mmol), TBHP (2.0 mmol), and solvent (1 mL).

only 10 min. The prepared catalyst is more reactive than $MoO_2Cl_2(dmf)_2$-MCM-41, MnII-L@CMK-3, and $MoO(O_2)_2(phox)/Fe_3O_4$ as reported by Monteiro [28], Mavrogiorgou [12] and Zare [38], respectively. Thus, the as prepared magnetic catalyst is more effective than the outlined catalysts for the studied reaction. Magnetic separation is another advantage of the reported catalyst.

3.3. Recyclability of the catalyst

Supported catalysts are usually prepared via complicated and expensive routes. Therefore, recycling of the used catalyst must be noted from an economical point of view. In the present work, the reusability of the supported Mo(VI) complex is checked in the epoxidation reaction of cyclooctene, as model substrates. After completion of the reaction the NPs were easily recovered by simple magnetic decantation, washed with absolute ethanol, dried in vacuum and re-used under the optimal conditions. As can be seen in Fig. 11, the supported catalyst can be reused at least three times with only a small loss of catalytic activity and without any change in selectivity. This experiment revealed that the obtained supported complex is a highly active nanocatalyst whichcan be re-used under the described reaction conditions.

4. Conclusions

In summary, the synthesis and characterization of a silane compound (TMOS-BIRD) for silylation of magnetite nanoparticles have been reported. $MoO_2Cl_2(dmf)_2$ was then supported onto MNP@BIRD to give a magnetically retrievable supported Mo^{6+} catalyst. The as-prepared magnetic catalyst was fully characterized by conventional methods and then successfully used for epoxidation reaction of alkenes in the presence of *t*-BuOOH as oxidant under solvent-free conditions. The applied catalyst could easily be retrieved from the reaction mixture through magnetic separation and then reused.

Acknowledgement

The Graduate Council of the University of Mohaghegh Ardabili is gratefully acknowledged for their financial support.

Table 3. Epoxidation reaction of olefins with TBHP catalysed by the supported Mo^{6+} complex under solvent-free condition.[a]

Entry	Olefin	Product(s)	Yield (%)	Selectivity (%)	TON	TOF (h^{-1})
1	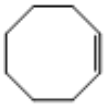	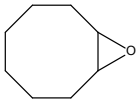	97.3	100	64.0	383.3
2		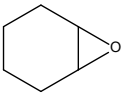	8.0	100	5.3	31.5
3	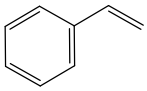	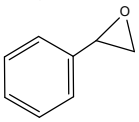	22.3	94.0 [b]	14.7	87.9
4	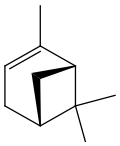	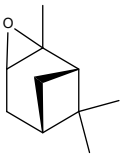	35.4	100	23.3	139.5
5	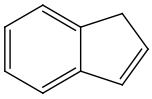	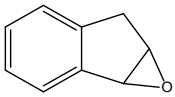	12.2	57.0 [c]	8.0	48.1
6	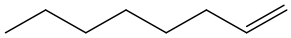	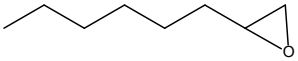	5.3	100	3.5	20.9
7	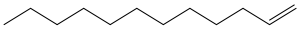	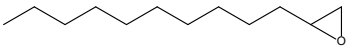	4.1	100	2.7	16.3
8	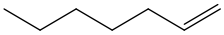	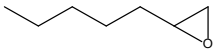	31.0	100	20.4	122.1
9	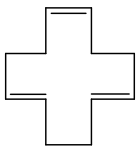	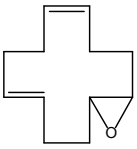	60.3	70 [d]	39.7	237.6
10	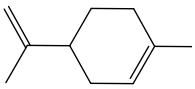	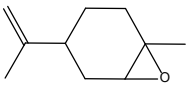	32.3	75 [e]	21.3	127.2
11	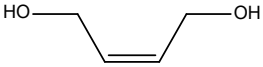	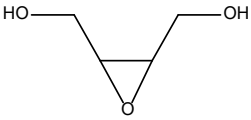	56.1	100	36.9	221.0
12	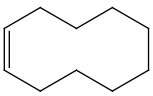	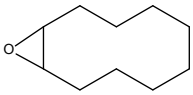	51.2	100	33.7	201.7

[a] Reaction conditions: Olefin (1.0 mmol), TBHP (2.0 mmol), Catalyst (1.5 mol%), Temperature (95 °C).

[b] Styrene oxide (94%) is the desired product and acetophenone (6%) is the by-product.

[c] Indene oxide (57%) is the desired product and 1H-Inden-1-one (43%) is the by-product.

[d] 1,2-Epoxy-5,9-cyclododecadiene (57%) is the desired product and diepoxide (1,2-epoxy-5,6-epoxy-9-cyclododecene, 30%) is the by-product.

[e] 1,2-Limonene oxide (75%) is the desired product and 1,2-8,9-limonene dioxide (25%) is the other product.

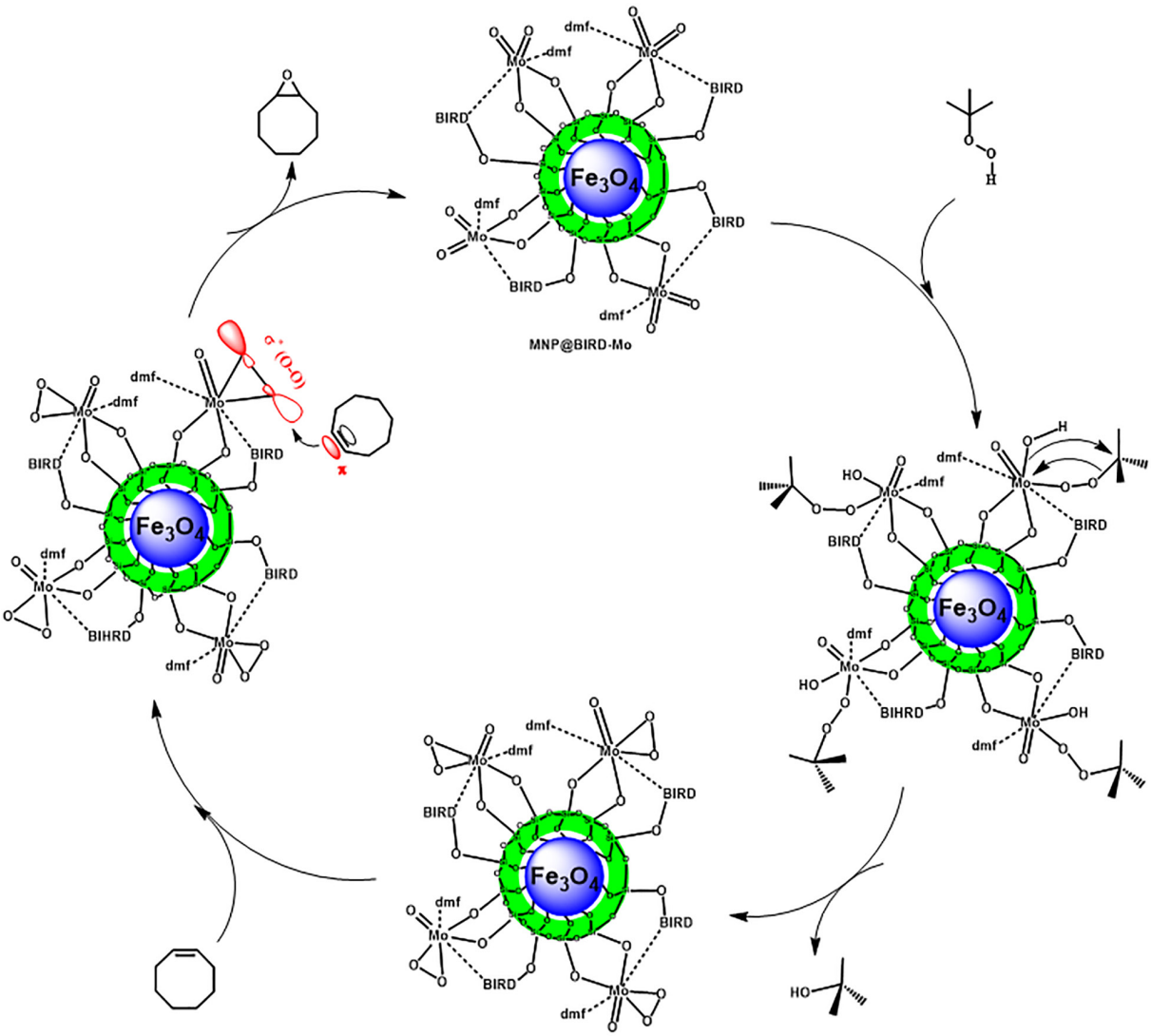

Scheme 3. Proposed mechanism for the epoxidation reaction of the olefins with supported Mo^{6+} catalyst.

Table 4. Comparison of the prepared catalyst with other catalysts for epoxidation reaction of cyclooctene.

Entry	Catalyst	Conditions	Time (min)	Yield (%)	TON/TOF (h^{-1})	Reference
1	$MoO_2Cl_2(dmf)_2$-MCM-41	TBHP / Solvent-free	360	100.0	91/544	[28]
2	$MoO(O_2)_2$(di-^{t}Bu-bipy)	TBHP / H_2O	24	98	98/4	[1]
3	$[MoO_2(SAP)]$	TBHP / Solvent-free	330	99.0	97/305	[39]
4	$[MoO_2(L_2)]_2$	TBHP / Solvent-free	240	86.0	346/344	[40]
5	$[MoO_2(NO_2)]_2$	TBHP / Solvent-free	240	86	346/86.5	[40]
6	Mn^{II}-L@CMK-3	$AcONH_4$, H_2O_2 / Acetone-MeOH	60	50.6	506/506	[12]
7	$MoO(O_2)_2$(phox) / Fe_3O_4	TBHP / Solvent-free	20	100.0	426/426	[38]
8	γ-Fe_2O_3@NaY	TBHP / CH_3CN	9	92	675/75	[41]
9	Ru^{3+}-Exchanged hydroxyapatite	O_2 / CH_3CN, *i*-butyraldehyde	2	94	19/9.5	[6]
10	Fe_3O_4@TMOS-BIRD-Mo	TBHP / Solvent-free	10	97.3	64/400	This work

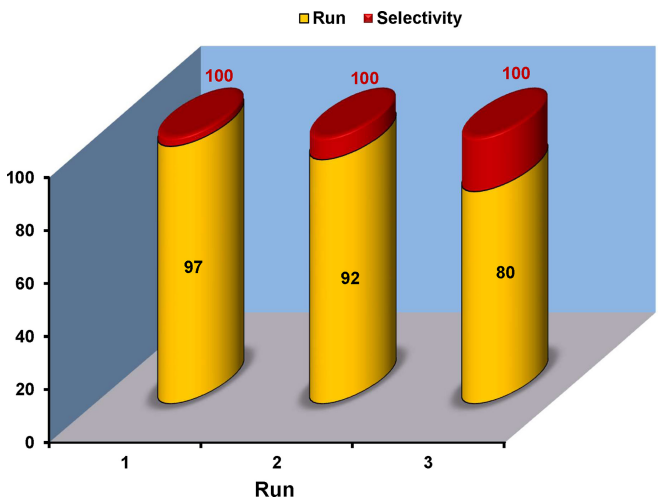

Fig. 11. Recycling of the supported Mo(VI) magnetic catalyst for the epoxidation reaction of cyclooctene with TBHP under optimal conditions.

References

[1] C.A. Gamelas, A.C. Gomes, S.M. Bruno, F.A.A. Paz, A.A. Valente, M. Pillinger, C.C. Romão, I.S. Gonçalves, Molybdenum (VI) catalysts obtained from η^3-allyl dicarbonyl precursors: Synthesis, characterization and catalytic performance in cyclooctene epoxidation, Dalton T. 41 (2012) 3474-3484.

[2] O.A. Wong, Y. Shi, Organocatalytic oxidation. Asymmetric epoxidation of olefins catalyzed by chiral ketones and iminium salts, Chem. Rev. 108 (2008) 3958-3987.

[3] M.L. Kuznetsov, J.C. Pessoa, Epoxidation of olefins catalysed by vanadium-salan complexes: a theoretical mechanistic study, Dalton T. (2009) 5460-5468.

[4] R. Dileep, B. Rudresha, An ionic liquid immobilized copper complex for catalytic epoxidation, RSC Adv. 5 (2015) 65870-65873.

[5] Z. Shi, C. Mei, G. Niu, Q. Han, Two inorganic-organic hybrids based on a polyoxometalate: Structures, characterizations, and epoxidation of olefins, J. Coord. Chem. 71 (2018) 1460-1468.

[6] Y. Uozumi, T. Osako, Olefin epoxidation on ruthenium-exchanged hydroxyapatite, Synfacts, 14 (2018) 0544.

[7] J. Zhang, P. Jiang, Y. Shen, W. Zhang, G. Bian, Covalent anchoring of Mo(VI) Schiff base complex into SBA-15 as a novel heterogeneous catalyst for enhanced alkene epoxidation, J. Porous Mat. 23 (2016) 431-440.

[8] A. Bezaatpour, E. Askarizadeh, S. Akbarpour, M. Amiria, B. Babaei, Green oxidation of sulfides in solvent-free condition by reusable novel Mo(VI) complex anchored on magnetite as a high-efficiency nanocatalyst with eco-friendly aqueous H_2O_2, Mol. Catal. 436 (2017) 199-209.

[9] S. Akbarpour, A. Bezaatpour, E. Askarizadeh, M. Amiri, Covalent supporting of novel dioxo-molybdenum tetradentate pyrrole-imine complex on Fe_3O_4 as high-efficiency nanocatalyst for selective epoxidation of olefins, Appl. Organomet. Chem. 31 (2017) e3804.

[10] N.E. Leadbeater, M. Marco, Preparation of polymer-supported ligands and metal complexes for use in catalysis, Chem. Rev. 102 (2002) 3217-3274.

[11] S.T. Firdovsi, M. Yagoub, A.E. Parvin, Transesterification reaction of dimethyl terephthalate by 2-ethylhexanol in the presence of heterogeneous catalysts under solvent-free condition, Chin. J. Chem. 25 (2007) 246-249.

[12] A. Mavrogiorgou, M. Baikousi, V. Costas, E. Mouzourakis, Y. Deligiannakis, M. Karakassides, M. Louloudi, Mn-Schiff base modified MCM-41, SBA-15 and CMK-3 NMs as single-site heterogeneous catalysts: Alkene epoxidation with H_2O_2 incorporation, J. Mol. Catal. A-Chem. 413 (2016) 40-55.

[13] P. Tayeb Oskoie, Y. Mansoori, Fe_3O_4@ZrO_2-SO_3H Nanoparticles for esterification of carboxylic acids, J. Part. Sci. Technol. 4 (2018) 1-12.

[14] H. Nagase, Studies on Fungicides. XXV. Addition reaction of dthiocarbamates to fumaronitrile, Bis (alkylthio) maleonitrile, 2,3-dicyano-5, 6-dihydro-1,4-dithiin and 4,5-dicyano-2-oxo-1,4-dithiole, Chem. Pharm. Bull. 22 (1974) 505-513.

[15] G. Baryshnikov, B. Minaev, V. Minaeva, H. Ågren, Theoretical study of the conformational structure and thermodynamic properties of 5-(4-oxo-1,3-thiazolidine-2-ylidene)-rhodanine and ethyl-5-(4-oxo-1,3-thiazolidine-2-ylidene)-rhodanine-3-acetic acid as acceptor groups of indoline dyes, J. Struct. Chem. 51 (2010) 817-823.

[16] K. Iijima, Y. Le Gal, T. Higashino, D. Lorcy, T. Mori, Birhodanines and their sulfur analogues for air-stable n-channel organic transistors, J. Mater. Chem. C, 5 (2017) 9121-9127.

[17] M. Rezaei, K. Azizi, K. Amani, Copper-birhodanine complex immobilized on Fe_3O_4 nanoparticles: DFT

studies and heterogeneous catalytic applications in the synthesis of propargylamines in aqueous medium, Appl. Organomet. Chem. 32 (2018) e4120.

[18] Z. Shahedi, Y. Mansoori, Fe_3O_4@SiO_2-SO_3H nanoparticles: An efficient magnetically retrievable catalyst for esterification reactions, J. Part. Sci. Technol. 4 (2018) 67-79.

[19] F. Nasiri, Y. Mansoori, N. Rostamzadeh, Novel polyesters and polyester/Cloisite 30B nanocomposites based on a new rhodanine-based monomer, Polym. Sci. Ser. B+, 59 (2017) 268-280.

[20] E. Subasi, A. Ercag, S. Sert, O.S. Senturk, Photochemical complexation reactions of $M(CO)_6$ (M = Cr, Mo, W) and $Re(CO)_5Br$ with rhodanine (4-thiazolidinone-2-thioxo) and 5-substituted rhodanines, Synth. React. Inorg. M. 36 (2006) 705-711.

[21] S. Rastegarzadeh, N. Pourreza, A.R. Kiasat, H. Yahyavi, Selective solid phase extraction of palladium by adsorption of its 5(p-dimethylaminobenzylidene) rhodanine complex on silica-PEG as a new adsorbent, Microchim. Acta 170 (2010) 135-140.

[22] A. Saxena, R. Upadhyay, Chemistry of the thiazolidinone alone or along with thiourea substituted amine complexes of Zinc (II), Orient. J. Chem. 28 (2012) 599-601.

[23] S. Seraj, B. Mirzayi, A. Nematollahzadeh, Superparamagnetic maghemite/polyrhodanine core/shell nanoparticles: Synthesis and characterization, Adv. Powder Technol. 25 (2014) 1520-1526.

[24] Y. Chen, S. Han, S. Yang, Q. Pu, Rhodanine stabilized gold nanoparticles for sensitive and selective detection of mercury(II), Dyes Pigments, 142 (2017) 126-131.

[25] A. Rahmaninia, Y. Mansoori, F. Nasiri, Surface-initiated atom transfer radical polymerization of a new rhodanine-based monomer for rapid magnetic removal of Co(II) ions from aqueous solutions, Polym. Adv. Technol. 29 (2018) 1988-2001.

[26] F. Nasiri, A. Zolali, S. Asadbegi, Solvent-free one-pot synthesis of 2,2′-dithioxo-[5,5′] bithiazolidinylidene-4,4′-diones, J. Heterocyclic Chem. 53 (2016) 989-992.

[27] F. Nasiri, P. Nazari, One-pot solvent-free three-component reaction between primary amines, carbon disulfide, and 5-alkylidene rhodanines: a convenient synthesis of asymmetric birhodanines, Mol. Divers. 22 (2018) 601-608.

[28] B. Monteiro, S.S. Balula, S. Gago, C. Grosso, S. Figueiredo, A.D. Lopes, A.A. Valente, M. Pillinger, J. P. Lourenço, I.S. Gonçalves, Comparison of liquid-phase olefin epoxidation catalysed by dichlorobis-(dimethylformamide) dioxomolybdenum (VI) in homogeneous phase and grafted onto MCM-41, J. Mol. Catal. A-Chem. 297 (2009) 110-117.

[29] Y. Mansoori, A. Khodayari, A. Banaei, M. Mirzaeinejad, Y. Azizian-Kalandaragh, M. Pooresmaeil, Fe_3O_4-PVAc nanocomposites: surface modification of sonochemically prepared magnetite nanoparticles via chemical grafting of poly (vinyl acetate), RSC Adv. 6 (2016) 48676-48683.

[30] A. Alizadeh, S. Rostamnia, N. Zohreh, R. Hosseinpour, A simple and effective approach to the synthesis of rhodanine derivatives via three-component reactions in water, Tetrahedron Lett. 50 (2009) 1533-1535.

[31] M. Mirzaeinejad, Y. Mansoori, M. Amiri, Amino functionalized ATRP-prepared polyacrylamide-g-magnetite nanoparticles for the effective removal of Cu(II) ions: Kinetics investigations, Mater. Chem. Phys. 205 (2018) 195-205.

[32] G.R. Ferreira, T. Segura, F.G. de Souza Jr, A.P. Umpierre, F. Machado, Synthesis of poly (vinyl acetate)-based magnetic polymer microparticles, Eur. Polym. J. 48 (2012) 2050-2069.

[33] J. Topich, Ligand control of the redox properties of dioxomolybdenum(VI) coordination complexes, Inorg. Chem. 20 (1981) 3704-3707.

[34] J.D. Hanawalt, H.W. Rinn, L.K. Frevel, Chemical Analysis by X-Ray Diffraction, Ind. Eng. Chem. Anal. Ed. 10 (1938) 457-512.

[35] J. Choubey, A.K. Bajpai, Investigation on magnetically controlled delivery of doxorubicin from superparamagnetic nanocarriers of gelatin crosslinked with genipin, J. Mater. Sci. Mater. M. 21 (2010) 1573-1586.

[36] C. Basavaraja, E.A. Jo, D.S. Huh, Characterization and magnetic properties of conducting poly(N-vinylcarbazole)-capped magnetite nanocomposite Langmuir-Schaefer films, Mater. Lett. 64 (2010) 762-764.

[37] B. Babaei, A. Bezaatpour, M. Amiri, S. Szunerits, R. Boukherroub, Magnetically reusable $MnFe_2O_4$ nanoparticles modified with oxo-peroxo Mo(VI) Schiff base complexes: A high efficiency catalyst for olefin epoxidation under solvent-free conditions,

ChemistrySelect, 3 (2018) 2877-2881.

[38] M. Zare, Z. Moradi-Shoeili, M. Bagherzadeh, S. Akbayrak, S. Özkar, Immobilization of a molybdenum complex on the surface of magnetic nanoparticles for the catalytic epoxidation of olefins, New J. Chem., 40 (2016) 1580-1586.

[39] J. Morlot, N. Uyttebroeck, D. Agustin, R. Poli, Solvent-free epoxidation of olefins catalyzed by "[MoO_2 (SAP)]": A new mode of *tert*-butylhydroperoxide activation, ChemCatChem, 5 (2013) 601-611.

[40] W. Wang, T. Guerrero, S.R. Merecias, H. García-Ortega, R. Santillan, J.-C. Daran, N. Farfán, D. Agustin, R. Poli, Substituent effects on solvent-free epoxidation catalyzed by dioxomolybdenum(VI) complexes supported by ONO Schiff base ligands, Inorg. Chim. Acta 431 (2015) 176-183.

[41] A. Blanckenberg, R. Malgas-Enus, Olefin epoxidation with metal-based nanocatalysts, Catal. Rev. 61 (2019) 27-83.